LETTER

doi:10.1038/nature09790

Aberrant chromosome morphology in human cells defective for Holliday junction resolution

Thomas Wechsler[1]†, Scott Newman[2] & Stephen C. West[1]

In somatic cells, Holliday junctions can be formed between sister chromatids during the recombinational repair of DNA breaks or after replication fork demise. A variety of processes act upon Holliday junctions to remove them from DNA, in events that are critical for proper chromosome segregation. In human cells, the BLM protein, inactivated in individuals with Bloom's syndrome, acts in combination with topoisomerase IIIα, RMI1 and RMI2 (BTR complex) to promote the dissolution of double Holliday junctions[1,2]. Cells defective for BLM exhibit elevated levels of sister chromatid exchanges (SCEs) and patients with Bloom's syndrome develop a broad spectrum of early-onset cancers caused by chromosome instability[3]. MUS81–EME1 (refs 4–7), SLX1–SLX4 (refs 8–11) and GEN1 (refs 12, 13) also process Holliday junctions but, in contrast to the BTR complex, do so by endonucleolytic cleavage. Here we deplete these nucleases from Bloom's syndrome cells to analyse human cells compromised for the known Holliday junction dissolution/resolution pathways. We show that depletion of MUS81 and GEN1, or SLX4 and GEN1, from Bloom's syndrome cells results in severe chromosome abnormalities, such that sister chromatids remain interlinked in a side-by-side arrangement and the chromosomes are elongated and segmented. Our results indicate that normally replicating human cells require Holliday junction processing activities to prevent sister chromatid entanglements and thereby ensure accurate chromosome condensation. This phenotype was not apparent when both MUS81 and SLX4 were depleted from Bloom's syndrome cells, suggesting that GEN1 can compensate for their absence. Additionally, we show that depletion of MUS81 or SLX4 reduces the high frequency of SCEs in Bloom's syndrome cells, indicating that MUS81 and SLX4 promote SCE formation, in events that may ultimately drive the chromosome instabilities that underpin early-onset cancers associated with Bloom's syndrome.

Our current understanding of the way in which Holliday junctions are processed in somatic cells suggests the three potential pathways illustrated in Supplementary Fig. 1. These include the dissolution of double Holliday junctions by BLM–TOPIIIα–RMI1–RMI2 (BTR), which suppresses crossover formation between sister chromatids[1], and the nucleolytic resolution of Holliday junctions by MUS81–EME1 (ref. 7) or GEN1 (ref. 12) that can lead to crossover or non-crossover products depending on the orientation of Holliday junction cleavage. Recently, it was shown that SLX4, a component of the SLX1–SLX4 nuclease complex that can also cleave Holliday junctions, associates with MUS81–EME1 and may provide a 'scaffold' function for several nuclease activities[8–11].

The relative contribution of each Holliday junction processing pathway is currently unknown. However, given that intact Holliday junctions are a relatively poor substrate for MUS81–EME1 (refs 4, 5), it is likely that the BTR complex provides the primary mechanism for the resolution of double Holliday junctions in human somatic cells at S phase. A further possibility is that resolution events mediated by MUS81–EME1, SLX1–SLX4 and/or GEN1 could substitute for the loss of BTR activity in Bloom's syndrome cells, either by cleaving the double Holliday junctions or other recombination intermediate structures (such as nicked Holliday junctions[14,15]), and thereby contribute to their viability.

Because nucleolytic cleavage mechanisms may be responsible for the elevated frequency of SCEs observed in Bloom's syndrome cells, we analysed SCE formation in metaphase spreads from the SV40-transformed Bloom's syndrome cell line GM08505 after short interfering RNA (siRNA)-mediated depletion of MUS81, SLX4 or GEN1. In all cases, efficient gene silencing was achieved, as measured by western blotting or quantitative reverse transcription PCR (RT–PCR) (Supplementary Fig. 2). Because depletion of SLX4 also decreases the levels of SLX1 (ref. 10), as the stabilities of SLX1 and SLX4 are interdependent, the SLX4 depletion should be viewed as an SLX1–SLX4 depletion. Depletion of SLX4 does not affect the levels of MUS81 or EME1 (ref. 10), or GEN1 (data not shown). We found that siRNA treatment against MUS81 or SLX4, but not GEN1, significantly reduced the frequency of SCEs (Fig. 1a, b), as well as the formation of harlequin chromosomes (that is, chromosomes exhibiting more than five SCEs) (Supplementary Fig. 3).

Although the SCE frequency in cells depleted for both MUS81 and GEN1 did not appear significantly different from MUS81-depleted cells, at least in metaphases that could be easily scored, many metaphase chromosomes looked abnormal after treatment with these siRNAs. Because these metaphases could not be scored for SCEs, it is possible that our scoring was biased towards those with only mild GEN1 and/or MUS81 depletion. We also observed decreased cell viability after dual siRNA treatment against GEN1 and MUS81, MUS81 and SLX4, or GEN1 and SLX4 (Fig. 1c), indicating that loss of multiple Holliday junction processing pathways can lead to cell death even in the absence of exogenous DNA damage. Depletion of GEN1 with SLX4, or MUS81 with SLX4, had a greater impact upon cell viability than GEN1 and MUS81 siRNA treatment, suggesting that SLX4 might have a broader role than either of the other nucleases.

When the chromosome aberrations seen in the metaphase spreads prepared from GEN1- and MUS81-depleted cells were analysed, we observed a high percentage of cells in which the chromosomes were elongated and segmented (Fig. 2a, compare left and right panels with enlargements below). Indeed, most chromosomes exhibited a 'beads-on-a-string' morphology. Similar results were obtained when the untransformed Bloom's syndrome fibroblast line GM01492 was treated with MUS81 and GEN1 siRNAs (Fig. 2b and Supplementary Fig. 4). Careful analysis of these spreads revealed the occasional appearance of single chromosomes that had an extreme defect in chromosome condensation (Fig. 2b, arrows).

These observations, with measurements showing that the total number of chromosomes in these metaphases was comparable to control spreads (data not shown), indicated that the beads-on-a-string morphology might result from an aberrant chromosome condensation defect rather than break-induced chromosome rearrangements. To confirm this, we performed whole chromosome painting on chromosomes 4, 8

[1]London Research Institute, Cancer Research UK, Clare Hall Laboratories, South Mimms, Hertfordshire EN6 3LD, UK. [2]Department of Pathology, University of Cambridge, Tennis Court Road, Cambridge CB2 1QP, UK. †Present address: Stanford University School of Medicine, Clark Center, 318 Campus Drive, Stanford, California 94305, USA.

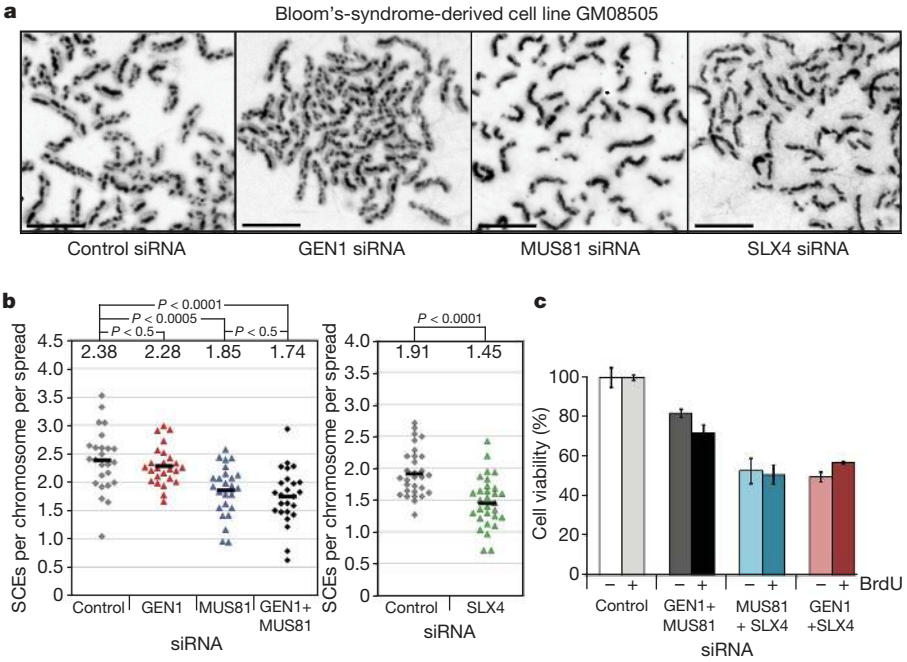

Figure 1 | Contribution of GEN1, MUS81 and SLX4 to SCE frequency in Bloom's syndrome cells. **a**, Representative images of metaphase spreads prepared from BLM-deficient GM08505 cells treated with the indicated siRNAs. Scale bars, 10 μm. **b**, Quantification of SCE frequency after siRNA treatment. Each data point represents a single cell/metaphase that was scored blind for SCEs per chromosome per spread (for each condition 25 cells, more than 1,700 chromosomes, were analysed). *P* values were determined using a two-tailed *t*-test. **c**, Relative cell viability measured 96 h after siRNA treatment that targeted two genes as indicated. Analyses were performed with and without BrdU treatment. Error bars, s.d.

and X in GM01492 Bloom's syndrome cells after GEN1 and MUS81 siRNA targeting. We found that segmentation occurred within intact chromosomes and was not due to translocation events (Fig. 2c). Indeed, although some chromosomal regions looked compact, others were more elongated and appeared as though held together by a thread of (non-staining) DNA. Our interpretation of the extended and segmented chromosome structure is that regions showing normal condensation are linked to uncondensed regions of DNA. Generally, the uncondensed

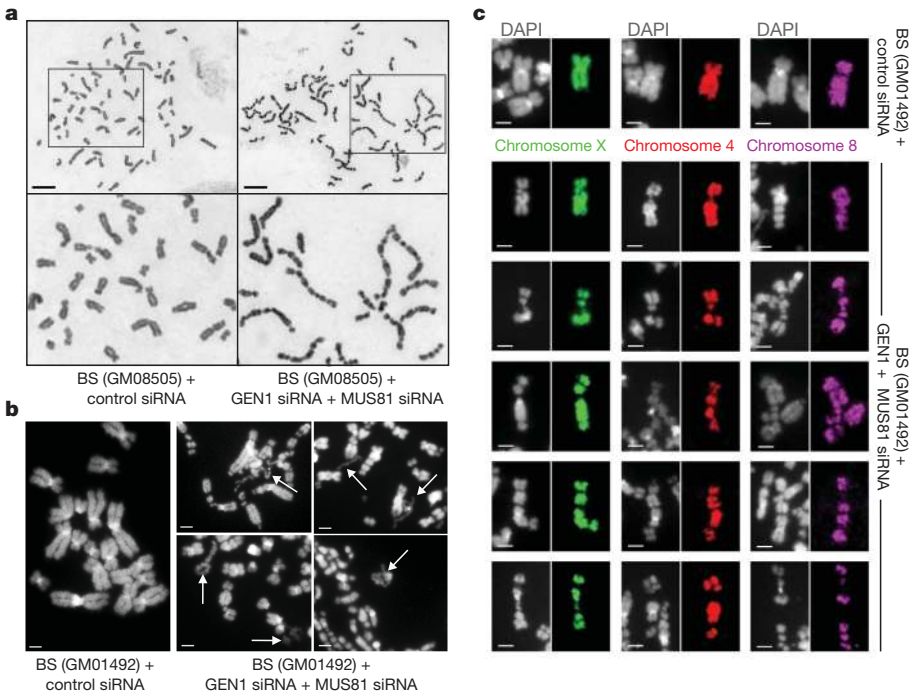

Figure 2 | Chromosome abnormalities in Bloom's syndrome (BS) cells after siRNA-mediated depletion of GEN1 and MUS81. **a**, Giemsa-stained metaphase spreads of GM08505 BLM-defective cells treated with control siRNA or siRNAs against both GEN1 and MUS81. The upper panels show whole chromosome spreads whereas the lower panels show the indicated sections at higher magnification. Scale bars, 10 μm. **b**, 4′,6-Diamidino-2-phenylindole (DAPI)-stained metaphase spreads of GM01492 BLM-defective cells treated with control siRNA or siRNAs against both GEN1 and MUS81 as indicated. White arrows indicate chromosomes with extreme condensation defects. Scale bars, 2 μm. **c**, Metaphase spreads from the experiment described in **b** were stained with whole chromosome paints specific for chromosome 4, 8 or X, as indicated. The selected chromosomes are representative of those from a total of nine metaphase spreads. Scale bars, 2 μm.

regions were observed at equivalent positions on each of the two sister chromatids, which themselves remained tightly associated along their entire length. One possibility is that the loss of Holliday junction processing activity results, either directly or indirectly, in sister chromatid entanglements that prohibit normal chromosome condensation.

To quantify the observed segmentation phenotype, we counted chromosomes with more than three segments ($S > 3$) and scored metaphases with two or more segmented chromosomes as '$S > 3$ positive' (Fig. 3a). Using this scoring method, a baseline of 2% was observed with the control GM08505 Bloom's syndrome cells, whereas cells depleted for MUS81 or GEN1 contained 6% and 8% of $S > 3$ chromosomes, respectively (Fig. 3b). In contrast, 56% of the Bloom's syndrome metaphases depleted for both GEN1 and MUS81 exhibited two or more $S > 3$ chromosomes (Fig. 3b, c). Moreover, in 13% of these cells, the $S > 3$ phenotype was so severe that virtually all chromosomes in the spread were affected (Fig. 2a). To enable the most simple quantification, these severely affected cells were designated '>9'. The abnormal phenotype was not influenced by the presence or absence of BrdU (an agent used in the earlier SCE analyses) (Supplementary Fig. 5). When the same scoring method was applied to the Bloom's syndrome cell line GM01492 after GEN1- and MUS81-depletion, we found that 46% of the cells (compared with 7% in control cells) showed an $S > 3$ phenotype, ruling out any cell-line-specific effects (Supplementary Fig. 4).

Importantly, the chromosome abnormalities observed in Bloom's syndrome cells depleted for both GEN1 and MUS81 were suppressed by exogenous expression of BLM protein, as shown by comparison of the BLM-defective cell line PSNG13 with its isogenic BLM-complemented cell line PSNF5 after GEN1 and MUS81 siRNA treatment (Fig. 3d–f and Supplementary Fig. 6). We also failed to observe an increase in $S > 3$ chromosomes in the BLM-proficient cell line U2OS, despite a high depletion efficiency of GEN1 and MUS81 (Supplementary Fig. 7). These results show that BLM is critical for the maintenance of genome stability, and that loss of Holliday junction processing activity caused by disruption of BLM, MUS81 and GEN1 leads to aberrant chromosome morphology.

In yeast, it has been shown that *yen1 mus81* double mutants (Yen1 is the yeast orthologue of GEN1) are considerably more sensitive to DNA damage than the *mus81* single mutant[16,17] and that Mus81 and Yen1 can promote crossover formation during mitotic recombination[18]. These studies indicate that recombination intermediates normally resolved by Mus81 can also serve as substrates for Yen1. In mammalian cells, however, we currently have little information relating to the interplay between GEN1 and MUS81, or with SLX4 with which MUS81 interacts[8–11]. Therefore, to gain our first insights into the genetic interactions between these proteins, we depleted combinations of either MUS81 + SLX4, GEN1 + SLX4 or, as before, GEN1 + MUS81, and measured the extent of chromosome aberrations. We found that depletion of GEN1 and SLX4 in Bloom's syndrome cells resulted in an extremely severe phenotype, as measured by the formation of segmented chromosomes (Fig. 4). The next most severe combination was caused by depletion of GEN1 and MUS81. In contrast, the chromosome abnormalities observed after siRNA treatment against both MUS81 and SLX4 were considerably less severe. These results favour the view that SLX4 plays a broad role, not only in a nuclease complex with SLX1, but also as a scaffold for the cooperative actions of other nucleases.

The severe phenotype observed after GEN1 and SLX4 depletion allowed us to perform two further experiments. First, time-course analyses revealed that $S > 3$ chromosomes were detectable 36 h after

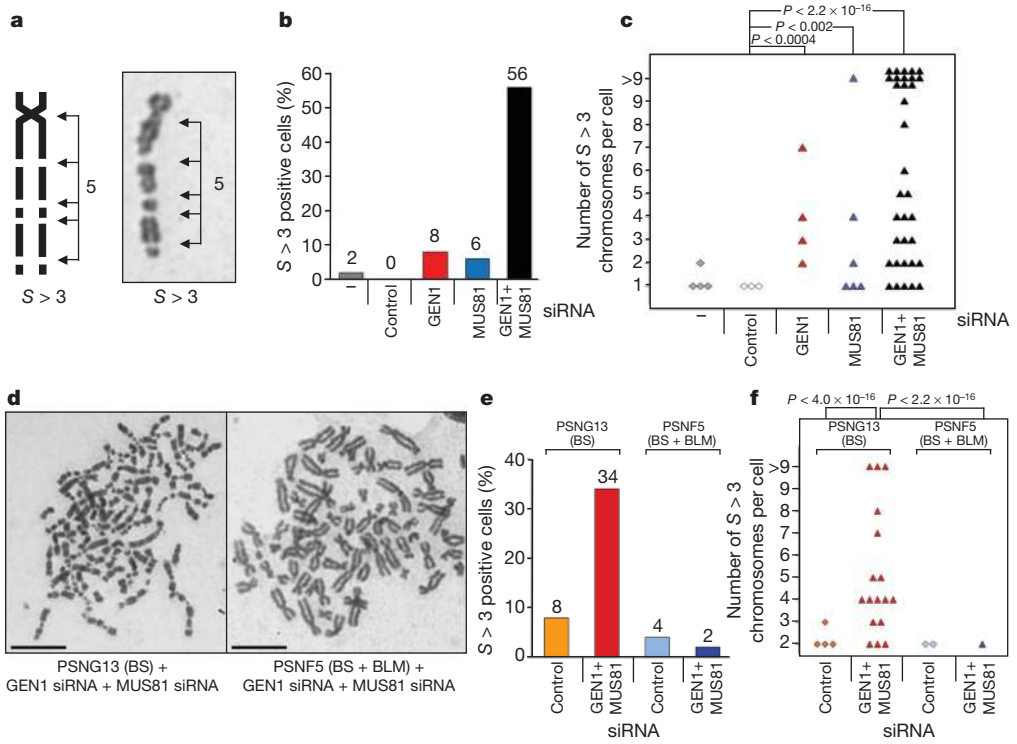

Figure 3 | Quantification of the chromosome segmentation phenotype observed in Bloom's syndrome cells after GEN1 and MUS81 depletion. **a**, Schematic illustration (left) and Giemsa staining (right) of an abnormal metaphase chromosome showing more than three indentations ($S > 3$). The definition $S > 3$ was used in all subsequent experiments. **b**, After the treatment of GM08505 Bloom's syndrome cells with the indicated siRNAs, metaphases ($n = 50$) were scored. The percentage of cells with at least two $S > 3$ chromosomes is shown. **c**, As **b** but to illustrate phenotypic severity, the number of $S > 3$ chromosomes in each metaphase ($n = 50$) was plotted in a scatter graph. Only metaphases with at least one $S > 3$ chromosome are shown, and those with more than nine segmented chromosomes were termed '>9'. **d**, Complementation of Bloom's syndrome cells with BLM restores chromosome stability. BLM-deficient PSNG13 and the BLM-complemented PNSF5 cell lines were treated with siRNA against GEN1 and MUS81, and analysed for abnormal metaphases using Giemsa staining. Scale bars, 10 μm. **e**, **f**, Metaphases ($n = 50$) were analysed after control or GEN1 + MUS81 siRNA treatment of PSNG13 and PSNF5 cells. Quantifications were performed as in Fig. 3b.

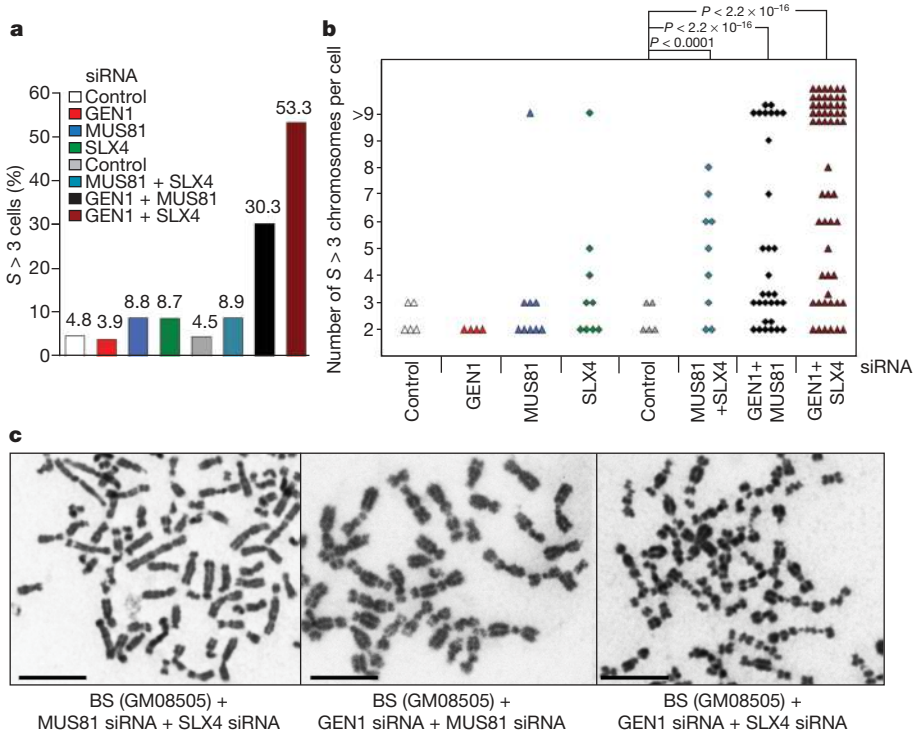

Figure 4 | Synthetic interactions between GEN1, MUS81 and SLX4. GM08505 Bloom's syndrome cells were depleted for GEN1, MUS81 or SLX4, or for the indicated pairs of proteins. Cells were collected 60 h after the second transfection and metaphase cells ($n > 100$) were scored (**a**, **b**) and visualized (**c**) as in Fig. 3. Scale bars, 10 μm.

siRNA treatment, and that the severity of the abnormal chromosome phenotype continued into the second mitotic division (Supplementary Fig. 8). After this point, high levels of cell inviability were observed (Fig. 1c). Second, we found that the chromosome indentations were effectively free of SMC2 protein, confirming that the unusual phenotype was indeed due to a defect in proper chromosome condensation (Supplementary Fig. 9).

These results begin to define the relative contributions of GEN1, MUS81 and SLX4 to Holliday junction processing in human mitotic cells already defective for BLM. Inactivation of MUS81, together with GEN1, effectively produces BLM-defective cells compromised for the known Holliday junction dissolution/resolution pathways. The resulting phenotype was the formation of highly segmented chromosomes with severe condensation defects. Similar results were observed by inactivation of GEN1 and SLX4, supporting the notion that SLX4 and MUS81 might work in the same pathway. Although this is the first time that such an aberrant chromosome morphology has been associated with defects in Holliday-junction processing, similar defects have been observed in human and mouse cells in response to ionizing radiation which causes a delay in DNA replication timing that, in turn, affects mitotic chromosome condensation[19]. Similarly, defects in DNA replication due to the mutation of key replication factors such as ORC2 also lead to segmented chromosome condensation morphology. Together, these studies indicate a potential link between DNA replication and the establishment of proper chromosome condensation, and it has been suggested that the timely completion of replication impacts upon the lateral condensation of a metaphase chromosome by helping to remove entanglements[20]. In our study, we suggest that sister chromatid entanglements, caused instead by defects in Holliday junction processing pathways, might lead to a related aberrant condensation phenotype. The beads-on-a-string chromosome morphology seen here, and the absence of significant break-induced chromosome translocations, indicates that the regions of under-condensed chromatin retain fine DNA threads that link the normally condensed regions. Moreover, the tight side-by-side alignment of sister chromatids is suggestive of the persistence of unresolved bridges that accumulate after disruption of the three cellular Holliday junction processing pathways.

It has been shown that BLM protein localizes to ultrafine bridges at anaphase, and that these sites represent unresolved entanglements that occur at fragile sites after replication stress[21–23]. However, many ultrafine bridges derive from centromeric regions[21,24], whereas our work shows that the indentations corresponding to regions of under-condensed chromatin are distributed randomly along the length of each chromosome.

The aberrant chromosome morphology seen in the current experiments was suppressed by expression of the BLM protein, leading us to suggest that Holliday junction dissolution, a system that avoids SCEs, provides the primary mechanism for the processing of Holliday junctions in somatic cells. In the absence of this pathway, such as in cells derived from patients with Bloom's syndrome, elevated levels of SCEs are observed and we have shown that these can arise through the actions of MUS81 or SLX4. The precise role of SLX4 is currently unknown, as it may function either as a junction-specific nuclease with SLX1, or it may provide a scaffold for the cooperation of multiple nucleases within a multi-functional DNA processing complex. Loss of both BLM and MUS81 (or SLX4), however, did not result in a severe condensation phenotype, because mitotic cells possess a third pathway of Holliday junction resolution mediated by GEN1, for which we present the first functional evidence *in vivo*. It is likely that MUS81–EME1, SLX1–SLX4 and GEN1 can resolve Holliday junctions that persist in BLM-defective cells, although the bi-directional nature of their cleavage mechanism will, in contrast to the BTR complex, produce SCEs. We therefore suggest that the nucleolytic processing pathways provide additional mechanisms of resolution that can act upon intermediates that escape the attention of the BTR complex, thereby allowing chromosome segregation. Use of these alternatives may, however, come at a price because Bloom's syndrome cells exhibit genomic instability and patients suffer a broad spectrum of early-onset cancers.

METHODS SUMMARY

The human osteosarcoma cell line U2OS, SV40-transformed Bloom's syndrome fibroblasts GM08505 (ref. 25) and untransformed Bloom's syndrome fibroblasts GM01492 (ref. 26) were provided by CRUK Cell Services (Clare Hall). The cell line PSNF5 constitutively expresses BLM protein, whereas the isogenic control PSNG13 contains pcDNA3 vector DNA[27]. Cells were transfected twice with siRNA within 24 h. For a single gene, 3×10^5 cells were transfected with 400–500 pmol of siRNA (Dharmacon) using 10 µl of Lipofectamine RNAiMAX (Invitrogen). For double-gene targeting, up to 800 pmol of siRNA was mixed and transfected with 20 µl Lipofectamine. Control non-targeting siRNAs were used at equivalent concentrations. The efficiency of each siRNA treatment was monitored by western blotting 60 h after the first, or 36 h after the second, transfection, or by quantitative RT–PCR 48 h after the first treatment. SCEs and metaphase chromosomes were monitored as described[28,29]. The SCE technique relies upon the differential staining of the sister chromatids after replication in the presence of BrdU, followed by staining with Hoechst dye and Giemsa. Cell viability assays were performed 12 h after the second transfection with various siRNA combinations (MUS81 + SLX4; GEN1 + MUS81; GEN1 + SLX4). The cells were then seeded in equal numbers (2,000 per well) in a 96-well plate (in triplicates), grown for a further 84 h and tested using the Cell-Titre Glo assay system (Promega). Chromosome painting was performed as described[30].

Full Methods and any associated references are available in the online version of the paper at www.nature.com/nature.

Received 26 July 2010; accepted 5 January 2011.
Published online 13 March 2011.

1. Wu, L. & Hickson, I. D. The Bloom's syndrome helicase suppresses crossing over during homologous recombination. *Nature* **426,** 870–874 (2003).
2. Mankouri, H. W. & Hickson, I. D. The RecQ helicase-topoisomerase III-Rmi1 complex: a DNA structure-specific 'dissolvasome'? *Trends Biochem. Sci.* **32,** 538–546 (2007).
3. Bachrati, C. Z. & Hickson, I. D. RecQ helicases, suppressors of tumorigenesis and premature aging. *Biochem. J.* **374,** 577–606 (2003).
4. Chen, X. B. *et al.* Human MUS81-associated endonuclease cleaves Holliday junctions *in vitro*. *Mol. Cell* **8,** 1117–1127 (2001).
5. Ciccia, A., Constantinou, A. & West, S. C. Identification and characterization of the human MUS81/EME1 endonuclease. *J. Biol. Chem.* **278,** 25172–25178 (2003).
6. Ciccia, A., McDonald, N. & West, S. C. Structural and functional relationships of the XPF/MUS81 family of proteins. *Annu. Rev. Biochem.* **77,** 259–287 (2008).
7. Taylor, E. R. & McGowan, C. H. Cleavage mechanism of human MUS81–EME1 acting on Holliday-junction structures. *Proc. Natl Acad. Sci. USA* **105,** 3757–3762 (2008).
8. Andersen, S. L. *et al. Drosophila* MUS312 and the vertebrate ortholog BTBD12 interact with DNA structure-specific endonucleases in DNA repair and recombination. *Mol. Cell* **35,** 128–135 (2009).
9. Fekairi, S. *et al.* Human SLX4 is a Holliday junction resolvase subunit that binds multiple DNA repair/recombination endonucleases. *Cell* **138,** 78–89 (2009).
10. Munoz, I. M. *et al.* Coordination of structure-specific nucleases by human SLX4/BTBD12 is required for DNA repair. *Mol. Cell* **35,** 116–127 (2009).
11. Svendsen, J. M. *et al.* Mammalian BTBD12/SLX4 assembles a Holliday junction resolvase and is required for DNA repair. *Cell* **138,** 63–77 (2009).
12. Ip, S. C. Y. *et al.* Identification of Holliday junction resolvases from humans and yeast. *Nature* **456,** 357–361 (2008).
13. Rass, U. *et al.* Mechanism of Holliday junction resolution by the human GEN1 protein. *Genes Dev.* **24,** 1559–1569 (2010).
14. Osman, F., Dixon, J., Doe, C. L. & Whitby, M. C. Generating crossovers by resolution of nicked Holliday junctions: a role of Mus81–Eme1 in meiosis. *Mol. Cell* **12,** 761–774 (2003).
15. Gaillard, P.-H. L., Noguchi, E., Shanahan, P. & Russell, P. The endogenous Mus81–Eme1 complex resolves Holliday junctions by a nick and counternick mechanism. *Mol. Cell* **12,** 747–759 (2003).
16. Blanco, M. G., Matos, J., Rass, U., Ip, S. C. Y. & West, S. C. Functional overlap between the structure-specific nucleases Yen1 and Mus81-Mms4 for DNA damage repair in *S. cerevisiae*. *DNA Repair (Amst.)* **9,** 394–402 (2010).
17. Tay, Y. D. & Wu, L. Overlapping roles for Yen1 and Mus81 in cellular Holliday junction processing. *J. Biol. Chem.* **285,** 11427–11432 (2010).
18. Ho, C. K., Mazón, G., Lam, A. F. & Symington, L. S. Mus81 and Yen1 promote reciprocal exchange during mitotic recombination to maintain genome integrity in budding yeast. *Mol. Cell* **40,** 988–1000 (2011).
19. Breger, K. S., Smith, L., Turker, M. S. & Thayer, M. J. Ionizing radiation induces frequent translocations with delayed replication and condensation. *Cancer Res.* **64,** 8231–8238 (2004).
20. Hearst, J., Kauffman, L. & McClain, W. A simple mechanism for the avoidance of entanglement during chromosome replication. *Trends Genet.* **14,** 244–247 (1998).
21. Chan, K. L., North, P. S. & Hickson, I. D. BLM is required for faithful chromosome segregation and its localization defines a class of ultrafine anaphase bridges. *EMBO J.* **26,** 3397–3409 (2007).
22. Chan, K. L., Palmai-Pallag, T., Ying, S. M. & Hickson, I. D. Replication stress induces sister-chromatid bridging at fragile site loci in mitosis. *Nature Cell Biol.* **11,** 753–760 (2009).
23. Naim, V. & Rosselli, F. The FANC pathway and BLM collaborate during mitosis to prevent micro-nucleation and chromosome abnormalities. *Nature Cell Biol.* **11,** 761–768 (2009).
24. Baumann, C., Korner, R., Hofmann, K. & Nigg, E. A. PICH, a centromere-associated SNF2 family ATPase, is regulated by Plk1 and required for the spindle checkpoint. *Cell* **128,** 101–114 (2007).
25. Wu, L., Davies, S. L., Levitt, N. C. & Hickson, I. D. Potential role for the BLM helicase in recombinational repair via a conserved interaction with RAD51. *J. Biol. Chem.* **276,** 19375–19381 (2001).
26. Ellis, N. A., Proytcheva, M., Sanz, M. M., Ye, T.-Z. & German, J. Transfection of BLM into cultured Bloom syndrome cells reduced the sister-chromatid exchange rate toward normal. *Am. J. Hum. Genet.* **65,** 1368–1374 (1999).
27. Gaymes, T. J. *et al.* Increased error-prone non homologous DNA end-joining – a proposed mechanism of chromosomal instability in Bloom's syndrome. *Oncogene* **21,** 2525–2533 (2002).
28. Bender, C. F. *et al.* Cancer predisposition and hematopoietic failure in *Rad50*$^{(S/S)}$ mice. *Genes Dev.* **16,** 2237–2251 (2002).
29. Bayani, J. & Squire, J. A. Sister chromatid exchange. *Curr. Protoc. Cell Biol.* **22** 7, (2005).
30. Alsop, A. E., Teschendorff, A. E. & Edwards, P. A. W. Distribution of breakpoints on chromosome 18 in breast, colorectal, and pancreatic carcinoma cell lines. *Cancer Genet. Cytogenet.* **164,** 97–109 (2006).

Supplementary Information is linked to the online version of the paper at www.nature.com/nature.

Acknowledgements We thank I. Hickson for providing the Bloom's syndrome cell lines and advice, P. Edwards for help and providing facilities for chromosome painting, S. Horswell for the statistical analysis, S. Ip for the GEN1 antibody, M.G. Blanco for assistance with SCE scoring and our laboratory colleagues for their encouragement and suggestions. We further thank K. Cimprich, the Cimprich laboratory members, and C. Wang, W. Johnson and A. Straight. This work was supported by Cancer Research UK, the Louis-Jeantet Foundation, the European Research Council, the Swiss Bridge Foundation and the Breast Cancer Campaign. S.N. was supported by a studentship from the UK Medical Research Council.

Author Contributions T.W. and S.C.W. designed the project that was undertaken entirely by T.W. Expertise for the chromosome paints was provided by S.N. The manuscript was written by S.C.W. with help from T.W.

Author Information Reprints and permissions information is available at www.nature.com/reprints. The authors declare no competing financial interests. Readers are welcome to comment on the online version of this article at www.nature.com/nature. Correspondence and requests for materials should be addressed to S.C.W. (stephen.west@cancer.org.uk).

METHODS

Antibodies. Affinity-purified anti-GEN1 rabbit polyclonal antibody was raised against a carboxy (C)-terminal peptide (CLDSPLPLRQRLKLRFQST) corresponding to GEN1$^{890-908}$. Mouse monoclonal antibodies against MUS81 (2G10/3) and RAD51 (14B4) were purchased from Abcam, and rabbit polyclonal antibody against SMC2 (A300-058A) was from Bethyl Labs.

siRNA transfections, quantitative RT–PCR and western blotting. For siRNA transfections, 3×10^5 cells were seeded in 60 mm cell culture dishes 8 h before transfection. In general, the cells were transfected twice within 24 h and the cell culture medium was changed after the first transfection. For depletion of a single protein, 3×10^5 cells were transfected with 400–500 pmol of siRNA using 10 µl of Lipofectamine RNAiMAX (Invitrogen). For double targeting, up to 800 pmol of siRNA was mixed and transfected with 20 µl Lipofectamine RNAiMAX; ON TARGET-plus siRNAs specific for each gene and control non-targeting siRNAs were purchased from Dharmacon and were used at the same concentrations. The efficiency of each siRNA treatment was monitored by western blotting 60 h after the first transfection, or 36 h after the second, or by quantitative RT–PCR 48 h after the first transfection. The siRNA sequences, indicated 5′ to 3′, were as follows. Control siRNA: ON-TARGET*plus* non-targeting siRNA #3. GEN1/FLJ40869 oligonucleotides 1–4: (1) GCGUAAUCUUGGUGGGAAA; (2) UCUAAGACCU UUGGCUAUA; (3) UAUGCAAACCACUCGGAAA; (4) GCCCUAAGAUACA UAUUAA. SLX4 (oligonucleotides 1–2)[9–11]: (1) AAACGUGAAUGAAGCA GAAUU; (2) CGGCAUUUGAGUCUGCAGGUGAA. MUS81 (oligonucleotides 1–2): (1) CAGCCCUGGUGGAUCGAUA; (2) CAUUAAGUGUGGGCGUCUA.

Owing to the lack of specificity of SLX4 antibodies, the efficiency of depletion of SLX4 was determined by quantitative RT–PCR. For this, total RNA was isolated using the RNeasy kit (Qiagen) according to the manufacturer's instructions with the following modifications: cell lysis was achieved using QIAshredder columns (Qiagen) and DNase I treatment was performed before total RNA was eluted from the RNeasy column. Then 1 µg of total RNA was reverse transcribed using a TaqMan Reverse Transcription Kit (Applied Biosystems) in a 20-µl reaction and used for three quantitative RT–PCR reactions in a 96-well format using the EXPRESS SYBR GreenER qPCR SuperMix with Premixed ROX (Invitrogen) and a Real-Time PCR System (Applied Biosystems). The ribosomal protein L23 mRNA was used as a standard. Depletion of SLX4 (or SLX1) by siRNA treatment results in a loss of both SLX1 and SLX4, as their stabilities are interdependent[10]. Use of siRNAs against either is therefore considered to be equivalent to SLX1–SLX4 depletion.

Primers for quantitative RT–PCR of GEN1: forward, CCACATGACTATG AATACTGCTGTCCTT; backward, TGGGAATCCCTCACAACAGCAAGC.

Primers for quantitative RT–PCR of SLX4: forward, CCTGGAGGAAAA GGGTTTGT; backward, AGCTTCATCCAAGCACCTGT.

Primers for quantitative RT–PCR of L23: forward, TTCCTGGTCCACA ACGTCAAG; backward, TTGTGAAGCGATCTCGGCA.

Cell viability assays. Cells were collected 12 h after the second siRNA transfection with various siRNA combinations (MUS81 + SLX4; GEN1 + MUS81; GEN1 + SLX4). They were then seeded in equal numbers (2,000 per well) in 96-well plates in triplicates (with or without 66 µM BrdU) and incubated for 84 h. Cell viability was determined using the Cell-Titre Glo assay (Promega).

Analysis of metaphase chromosomes. For the SCE assay, 3×10^5 cells were seeded in 60-mM plates before siRNA transfection. After 8 h, the cells were transfected with siRNA, grown for a further 24 h and then transfected again. After 18 h growth, BrdU (100 µM) was added and the cells were grown for a further 60–72 h. Metaphase chromosomes were prepared and assayed for SCEs by a modification of published procedures[28,29]. Briefly, cells were incubated for 1 h with 0.2 µg ml^{-1} colcemid and metaphase cells were harvested by mitotic shake-off. The cells were then swollen in 75 mM KCl for 20 min, fixed with methanol:acetic acid (3:1) and spread. After treatment with Hoechst 33258 and ultraviolet treatment, images were acquired using a Zeiss Axio Imager M1 microscope using a Plan-Neofluar ×60, 0.4 numerical aperture oil objective lens, and captured using an ORCA-ER camera (Hamamatsu) controlled by Volocity 4.3.2 software (Improvision). At least 25 images were taken randomly from each condition. The files were renamed and each image (at least 1,700 chromosomes per condition) was scored blind to determine both the number of SCEs per chromosome and the number of harlequin chromosomes per metaphase spread.

To visualize the segmented chromosome phenotype, the same procedure was performed except that BrdU was omitted and the cells were stained in 7% Giemsa for 7 min immediately after spreading and drying. The $S > 3$ phenotype was scored, and spreads with two or more chromosomes exhibiting the $S > 3$ phenotype were considered positive. For the most severely affected metaphases, the count was stopped at 10 and designated '>9'.

SMC2 staining. Metaphase cells were collected as above, swollen in 1× PME (5 mM Pipes/NaOH pH 7.2, 5 mM NaCl, 5 mM $MgCl_2$, 1 mM EGTA), resuspended in lysis buffer (1× PME supplemented with protease inhibitors, 0.1% Triton-X, 1 mM ATP, 0.2 mM spermine, 0.5 mM spermidine and 10 µg ml^{-1} cytochalasin B) and lysed on ice using a dounce homogenizer. Lysates were layered onto sucrose gradients (30, 40, 50 and 60% sucrose in 1× PME) and spun for 30 min at 2,000*g*. The chromosomes were taken from the 40/50% and 50/60% interfaces, and fixed in 3.7% formaldehyde and then centrifuged (20 min at 4,000*g*) through a 40% glycerol cushion onto polylysine-treated coverslips. Then chromosomes were stained with anti-SMC2 antibody (1:300) and Alexa Fluor 488-coupled goat anti-rabbit secondary antibody (1:1,000) and mounted in Vectashield containing DAPI.

Statistical analysis. Sister chromatid exchange data was subjected to a Student's two-tailed *t*-test. For $S > 3$ data, the counts were analysed by analysis of deviance using the generalized linear model fitting function glm() with a Poisson approximation to the multinomial, followed by analysis of deviance using the anova() function with the χ^2 test, both performed in R 2.10.1 (for details see http://www.R-project.org).